Macromolecular Research, Vol. 21, No. 9, pp 987-994 (2013)
DOI 10.1007/s13233-013-1124-4

www.springer.com/13233
pISSN 1598-5032 eISSN 2092-7673

Enhanced Moisture Barrier Films Based on EVOH/Exfoliated Graphite (EGn) Nanocomposite Films by Solution Blending

Hyok Kwon[1], Dowan Kim[1], Jongchul Seo*[,1], and Haksoo Han[2]

[1]*Department of Packaging, Yonsei University, Wonju 220-710, Korea*
[2]*Department of Chemical and Biomolecular Engineering, Yonsei University, Seoul 120-749, Korea*

Received October 18, 2012; Revised January 9, 2013; Accepted January 15, 2013

Abstract: A series of ethyl-vinyl alcohol (EVOH) nanocomposite films with exfoliated graphite nanosheets (EGn) were prepared *via* a solution blending method and their physical and moisture barrier properties were investigated as a function of the EGn content. The physical properties were strongly dependent upon the chemical and morphological structures originating from the differences in EGn composition. The nanocomposite films showed no strong interactions between the polymer and EGn filler, and this resulted in poor dispersion in relatively high content EVOH/EGn nanocomposites. With increasing content of EGn particles, the water vapor transmission rate varied in the range of 1.29 to 3.14 cc/m^2/day and the water uptake greatly decreased from 9.1 to 3.4 wt%. The water resistance capacity of EVOH was greatly enhanced and moisture diffusion in the pure EVOH film was retarded by introducing the EGn. However, thermal stabilities were not improved by incorporating EGn due to the poor interaction between EVOH polymer chains and the EGn surface.

Keywords: ethylene-vinyl alcohol (EVOH), exfoliated graphite nanosheet, nanocomposite film, moisture barrier properties, interfacial interaction.

Introduction

Ethylene-vinyl alcohol (EVOH) copolymers are a family of semicrystalline random copolymers widely used in food packaging applications due to their outstanding oxygen and odor barrier properties as well as their high resistance to oils and organic vapors and high transparency.[1,2] However, their resistance to oils and organic vapors decreases somewhat as the polarity of the penetrating compound increases. For example, the resistance to linear and aromatic hydrocarbons is outstanding, but for ethanol and methanol it is low; EVOH may absorb up to about 12 % of ethanol.[1] In barrier packaging applications, the major drawback is their moisture sensitivity that causes a significant decrease in the gas barrier properties at high relative humidity. This comes from the hydroxyl group, -OH, which makes the polymer hydrophilic, attracting water molecules. Because of its moisture sensitivity, EVOH is usually incorporated into multilayered package structures as a buried inner layer, surrounded by hydrophobic materials such as polyolefins (in most cases, polyethylene and polypropylene).[1] Although these structures provide high barrier properties, these structures typically contain an adhesive, or tie layer, between the EVOH and the polyolefin to provide adequate adhesion between the polar EVOH and the nonpolar polyolefin. Due to complex multilayered structure and combination of heterogeneous materials, this inevitably results in high cost and difficulties in recycling and reusing the materials. Therefore, various researchers are promoting a continuous search for enhanced barrier materials by nanocomposites incorporating nanoclays as a filler,[2,3] polymer blending,[4] and surface modification with plasma source ion implantation.[5]

Comparing with conventional particulate composites, nanocomposites consisting of nanoscale fillers dispersed in a polymer matrix may exhibit remarkable property enhancements at low loading of nanofillers such as exfoliated nanoclays[2,3,6] and graphite nanoplatelets.[7,8] These improvements can be more importantly achieved by optimizing the dispersion, interface chemistry, and nanoscale morphology to take advantage of the enormous surface area per unit volume (*i.e.*, aspect ratio) that nanofillers have. Among the nanofillers, graphite is a layered material consisting of one-atom thick sheets of carbon.[7-9] Graphite is structurally analogous to layered structures and chemically analogous to carbon nanotubes, making graphite an attractive nanofiller in both scientific and industrial fields. Separating the graphite layers into graphite sheets with nanoscale thickness can yield the desirable high aspect ratio, making graphite an ideal candidate for developing functional and structural reinforced composites.

*Corresponding Author. E-mail: jcseo@yonsei.ac.kr

A number of studies have been performed on graphite-reinforced polymer nanocomposites.[10-14] Investigations have been performed on thermoplastic materials such as polystyrene,[10] poly(methyl methacrylate) (PMMA),[11] nylon,[12] polypropylene,[13] and thermoset materials such as epoxy resins.[14] To prepare polymer/graphite nanocomposites, the expansion/exfoliation of graphite and its dispersion in a polymer matrix are key factors in obtaining remarkable enhancements in the physical properties of nanocomposites.[9,15] Expansion of the layer spacing in graphite occurs *via* heat treatment or exposure to microwave radiation followed by mechanical grinding.[15,16] The obtained exfoliated graphite nanosheets (EGn) have been incorporated into polymers *via* solvent mixing,[14] *in situ* polymerization,[10,11] and melt processing.[14,17] Solvent blending methods have been used in several investigations for enhanced dispersion in a polymer matrix.[17]

In this work, we have focused on investigating the effect of EGn nanosheets for physical properties such as moisture barrier properties for EGn-incorporated EVOH films (EVOH/EGn nanocomposite films). EGn nanosheets were successfully prepared by the thermal expansion of sulfuric acid-based intercalated graphite, followed by ultrasonic treatment. Six different EVOH/EGn nanocomposite films were prepared *via* a simple solvent blending method, and their morphological structure, thermal, and moisture barrier properties were investigated as a function of EGn content.

Experimental

Materials. EVOH used in this study was a commercial product EVAL™, containing 32 mol% ethylene segments, kindly supplied by Kuraray (Tokyo, Japan). Expandable graphite powders (EXP-527, purity > 99%) are a sulfuric acid-based intercalated graphite, purchased from Hyundai Coma Co., Ltd. (Youngju, Korea) in the form of thick platelets.[18] Dimethyl formamide (DMF) was purchased from Duksan Chemical Co., Ltd. (Ansan, Korea). All reagents were used as received without further purification.

Preparation of Exfoliated Graphite Nanosheets (EGn). EGn powders were prepared according to the literature.[13,18] Briefly, expandable graphite powders were subjected to rapid heating at 1050 °C for 30 s to exfoliate into expanded graphite. The expansion ratio by rapid heating was about 800%. The expanded graphite powders were immersed in DMF and sonicated using an ultrasonicator (VCX 750, Sonics & Materials Co., Ltd., Korea) at 70 W for 5 h to further exfoliate into individual or bundles of graphite nanoplatelets. The resulting dispersion then was centrifuged and filtered and dried at 160 °C to yield exfoliated graphite nanosheets (EGn). Figure 1(a) and (b) show the SEM images of the ultrasonicated EGn particles in which the particles were completely fragmented, resulting in tiny graphite sheets with a thickness of 30-50 nm and a diameter of 2-20 μm (average diameter of 7.4 μm). Figure 1(b) confirms that the individual graphite nanosheet is not a single graphite nanosheet, *i.e.*, graphene, but rather consists of several layers of graphite sheets.[14] However, the as-prepared graphite nanosheets possess a high aspect ratio (width-to-thickness) of around 150-250.

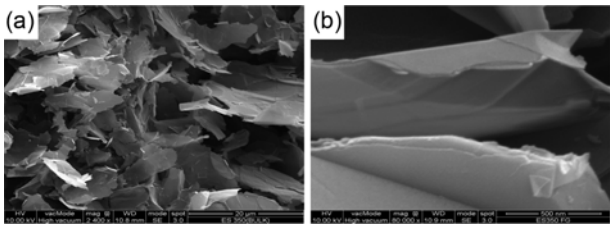

Figure 1. SEM images of the exfoliated graphite nanosheets (EGn): (a) Lower magnification and (b) higher magnification.

Preparation of the EVOH/EGn Nanocomposite Films. EVOH/EGn nanocomposite films with EGn loadings of 0-2 wt% were prepared as follows. EVOH (2 g) was dissolved in 30 mL of DMF at 50 °C. Then, certain amount of EGn powder was dispersed in DMF and ultrasonicated for 20 min. Next, this suspension of EGn was added to an EVOH solution, and the mixture was thoroughly mixed using an ultrasonicator for 2 h. To investigate the effect of EGn content on the properties of the nanocomposite films, we formulated EGn contents of 0, 0.1, 0.3, 0.5, 1, and 2 wt% with respect to the EVOH content. The obtained homogeneous solutions were slowly dropped and coated onto a glass plate, and then vacuum dried to a constant weight at 90 °C. The films were approximately 30 μm thick and were peeled off from the plate for other testing.

Characterization. Fourier transform infrared (FTIR) spectra of the as-prepared EVOH/EGn nanocomposite films were recorded with a Spectrum 65 FTIR spectrometer in attenuated total reflection (ATR) mode (PerkinElmer Co. Ltd., Massachusetts, USA). To analyze the morphologies of the EGn and nanocomposite films, wide angle X-ray diffraction (WAXD) patterns were obtained using a D/MAX-2500H X-ray diffractometer (Rigaku Co. Ltd., Tokyo, Japan) with a CuK_{α} (α=1.5406 Å) radiation source. The fractured surfaces of the nanocomposite films were obtained using a Nova 200 scanning electron microscope (SEM) (FEI Co. Ltd., Hillsboro, Oregon, USA). Prior to the examination, all of the samples were coated with a thin layer of platinum (Pt). The morphology of the EVOH/EGn nanocomposite films was also examined *via* transmission electron microscopy (TEM) with a Hitachi electron microscope. Samples for TEM analysis were sectioned with an ultramicrotome.

The decomposition temperature of the EVOH/EGn nanocomposite films were investigated by using a TGA 4000 thermogravimetric analyzer (PerkinElmer Co. Ltd., Massachusetts, USA) at a heating rate of 20 °C/min under a nitrogen atmosphere. Thermal behaviors of the nanocomposite films were investigated by means of a Q10 differential scan-

ning calorimeter (TA Instrument Co. Ltd., Delaware, USA) under a nitrogen atmosphere at a heating rate of 10 °C/min. All samples were heated to a temperature above their melting temperature (T_m), cooled at the same rate, and subsequently reheated. The thermal behaviors were determined from the second heating run.

For the moisture barrier properties of the EVOH/EGn nanocomposite films, their water vapor transmission rates (WVTR) were determined using a WVTR 7001 water vapor permeation analyzer (Systech Instruments Co. Ltd., Illinois, USA), according to ASTM F1249. The WVTR tests were carried out at 90 % relative humidity and 37.5 °C, and the data was directly obtained from the phosphorous pentoxide (P_2O_5) moisture sensor. In addition, the extent of water sorption of the nanocomposite films was determined gravimetrically. Before testing, each sample was dried in a vacuum oven at 60 °C for 24 h. First, the weight of each completely dried sample (W_d) was measured using a microbalance. Then, after the film was stored in a humidified chamber with deionized water for 24 h, each sample was removed, tapped with a moist Kim-wipe towel to remove the excess surface water, and was again weighed (W_s). Then, the water uptake (S) was calculated using the following equation:

$$S(\%) = (W_s - W_d)/W_d \times 100\ (\%)$$

The water contact angles on the EVOH/EGn nanocomposite films were measured using a Phoenix 300 contact angle goniometer (SEO Co. Ltd., Suwon, Korea). A droplet of water was gently placed on the film, and the average contact angle value was measured at five different locations for each sample. The droplets were observed through the eyepiece by applying the $\theta/2$ method and regulating the droplet size to about the 20 scale. Contact angles for the nanocomposite films were measured with definite time intervals for a single drop and the measurements were recorded as snap shots. To minimize the effect of evaporation on the water contact angle, all the measurements were conducted in a chamber controlled in the range of 80%-90% relative humidity.

Results and Discussion

Preparation of EVOH/EGn Nanocomposite. Strong interfacial and chemical interactions between polymer and inorganic components in composites are one of the most critical factors to improve their performance, and these can usually be identified through FTIR spectra analysis.[19-21] If a good interfacial interaction between the polymer matrix and inorganic components exists, an appreciable change and/or peak shift in the FTIR spectra of the composite films will be observed after adding each component. The FTIR spectra of a pure EVOH film and five different EVOH/EGn nanocomposite films are shown in Figure 2. In the IR spectrum of EVOH (Figure 1(a)), the characteristic bands assigned to methylene (CH_2) and methane (CH_3) stretching and deformation vibrations were present in the 2800-3000 and 1300-1500 cm^{-1} ranges, respectively. The intense band at 3100-3600 cm^{-1} was due to hydroxyl groups in the polymeric unit. As shown in Figure 1(b)-(f), the EVOH/EGn nanocomposite films showed similar IR spectra to pure EVOH, and no apparent change or shift in the characteristic peaks of pure EVOH was observed with the addition of EGn particles. This indicates poor interfacial interaction between the EVOH and EGn. EGn particles prepared by thermal expansion at 1,050 °C are generally nonpolar and thus have no strong self-interaction and do not agglomerate, as shown in the SEM images (Figure 1(a)). EGn also consists of only carbon, and has no functional groups that can interact with hydrophilic EVOH with hydroxyl groups, which may impede the chemical interaction between EGn and the EVOH matrix.[22,23] Thus, no change or shift in the characteristic IR peak was observed.

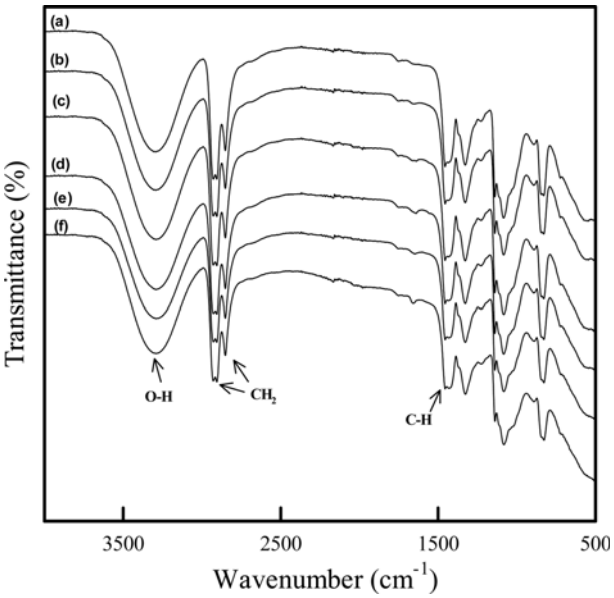

Figure 2. FTIR spectra of the EVOH/EGn nanocomposite films.

The morphology of the EVOH/EGn nanocomposite films, which ultimately affects their physical properties, including thermal stability, mechanical properties, and barrier properties, is strongly dependent upon the chemical composition.[10,13,17] The morphology of the EVOH/EGn nanocomposite films was investigated *via* SEM, TEM, and WAXD.

The dispersion status of EGn particles in the polymer matrix was observed using SEM. Figure 3 shows the fractured surface images of the EVOH/EGn nanocomposite films. The fractured surface of the pure EVOH film is slightly uneven and rough, indicating typical ductile failure. Similarly, EVOH/EGn nanocomposite films with 0.1%-0.5% EGn also exhibited a similar surface without any aggregation of the EGn sheets. Most of the EGn were well dispersed horizontally in the EVOH matrix (Figure 3(b)-(d)). Alternatively, it was noticeable that some cavities and agglomerations were

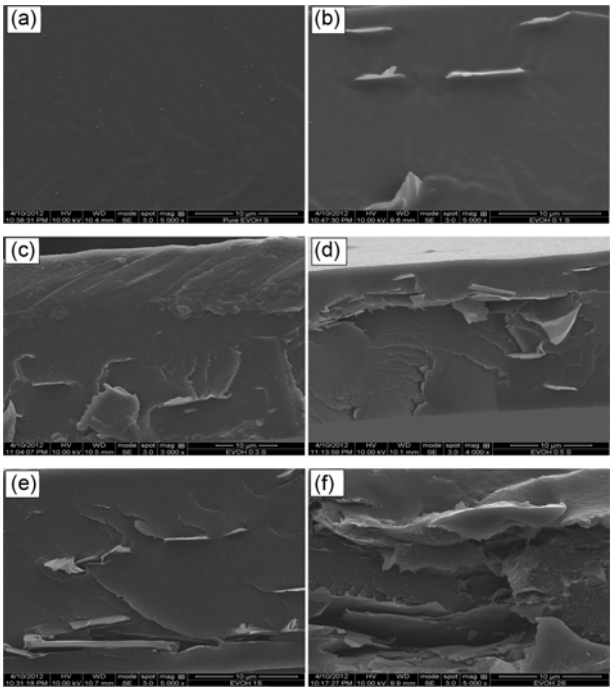

Figure 3. SEM images of the EVOH/EGn nanocomposite films with different contents of EGn: (a) 0%, (b) 0.1%, (c) 0.3%, (d) 0.5%, (e) 1%, and (f) 2%.

seen from the fractured surface of the EVOH/EGn 2% nanocomposite film. Furthermore, Figures 3(e) and (f) show that they easily separated from the EVOH matrix when the EVOH/EGn nanocomposite films were broken to produce a cross-section. This implies that the interfacial interaction between EVOH and EGn is not strong, which corresponds to the FTIR result. In other words, this can easily produce inner cracks and voids in the films, which may inhibit desirable physical properties. The morphological change in the EVOH matrix due to EGn particle loading may affect the physical properties of the EVOH/EGn nanocomposite films.[24]

Figure 4(a) shows TEM micrograph images of an EVOH/EGn 1% nanocomposite film. Although the graphite nanosheets are well dispersed in EVOH matrix, some graphite nanosheets are bridged or overlapped as shown in Figure 4(a). Figure 4(b) indicates that the graphite nanosheet is composed of several stacked individual graphite sheets of 3-8 nm thickness, and the total thickness is about 40 nm. This is consistent with the thickness of EGn nanosheets obtained by SEM, as shown in Figure 1. As shown in Figure 4(b), however, the agglomerations of EGn nanosheets in EVOH matrix are more noticeable for EVOH/EGn 2 % nanocomposite film.

Figure 5 shows the WAXD pattern of EGn powder (a) and those of the EVOH/EGn nanocomposite films (b), respectively. EGn showed one broad amorphous halo in the range of 15° to 25° (*d*-value is 3.64-5.95 Å). Additionally, it exhibited one sharp diffraction peak at 2θ=26.6° (*d*-value 3.46 Å) and one broad and less intense peak at 54.6° ((004) plane),

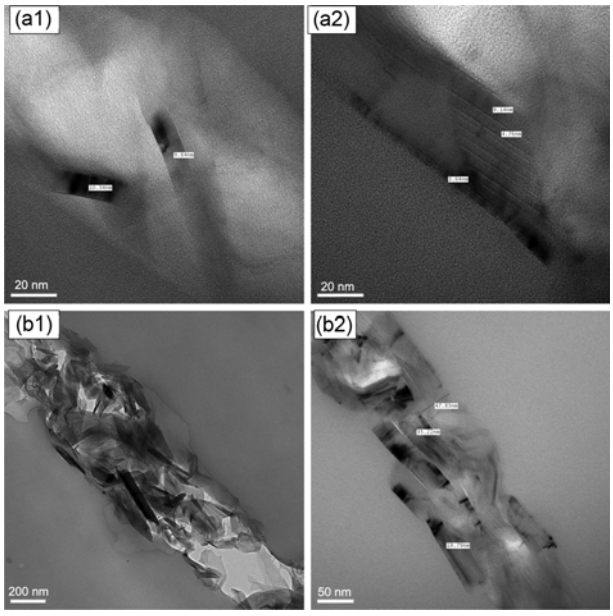

Figure 4. TEM images of the EVOH/EGn nanocomposite films with different contents of EGn: (a) 1% and (b) 2%.

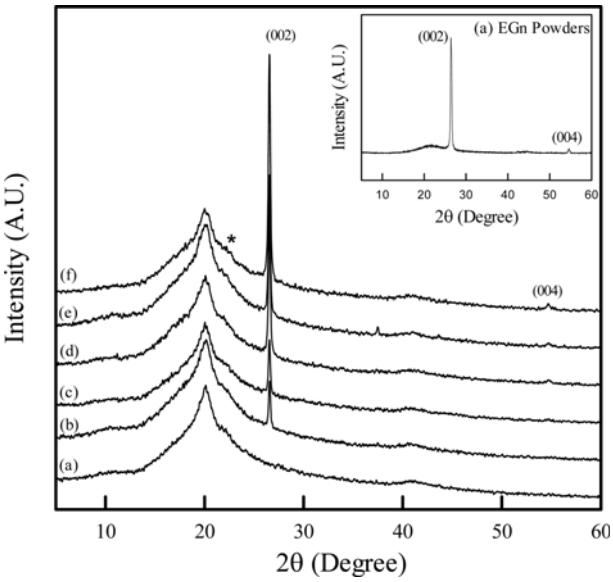

Figure 5. WAXD patterns of (a) EGn powders and (b)-(g) EVOH/EGn nanocomposite films.

which are consistent with graphite intercalation compounds.[25,26] Comparing with pure expandable graphite, however, a new amorphous halo appeared, and two characteristic peaks were weakened by the thermal expansion.[11,25] This indicates that the layer space was widened and the well-ordered graphite structure was largely collapsed by the thermal expansion process.

Meanwhile, pure EVOH showed one broad diffraction peak at 15°-25° and a weak diffraction peak around 41°, which were consistent with those reported in the literature.[27]

All the EVOH/EGn nanocomposite films showed a broad and non-crystalline peak of pure EVOH at 15°-25° with a shoulder around 22°, and two diffraction peaks: one strong peak at 26.4° and another slight indication at 54.6°. These two diffraction peaks and a shoulder on the amorphous halo apparently increased with increasing EGn content, and should be attributable to the graphite.[7] In contrast, the amorphous halo at 15°-25°, indicating the amorphous phase of pure EVOH, did not change. Apparently, the incorporation of EGn nanosheets into an EVOH matrix did not produce new peaks or peak shift with respect to pure EVOH. These WAXD results indicate that the incorporation of EGn particles does not alter the structural regularity of the base polymer and the EVOH/EGn nanocomposite films consist of two phases: polymer and EGn particles.

Thermal Properties. In general, the introduction of inorganic fillers, especially high aspect ratio fillers, into polymers can increase thermal stability.[28,29] Dynamic scanning calorimetry (DSC) and thermal gravimetric analysis (TGA) analyses were performed in a nitrogen atmosphere to investigate how the EGn content affects the thermal stability and thermal behaviors of the EVOH/EGn nanocomposite films. Their thermograms are depicted in Figures 6 and 7, respectively. Their transition temperatures and melting enthalpies were calculated from those thermograms and are summarized in Table I.

DSC curves of pure EVOH and EVOH/EGn nanocomposite films are shown in Figure 6, showing second heating run. In general, the thermal properties such as glass transition and melting temperatures are strongly associated with the mobility of the polymer chains.[7,8] The inorganic filler can serve to increase the glass transition temperature by decreasing the mobility of the polymer chains close to the filler surface. The physical confinement and strong interactions between polymer chains and the filler surface are two dominant contributions that affect chain mobility. However, regardless of the EGn content, all the nanocomposite films showed similar DSC patterns and no obvious changes in transitions and peaks. The glass transition temperature and melting temperature of EVOH are not changed by adding EGn into EVOH during the second heating run in DSC, indicating that the interfacial interaction between EVOH polymer chains and

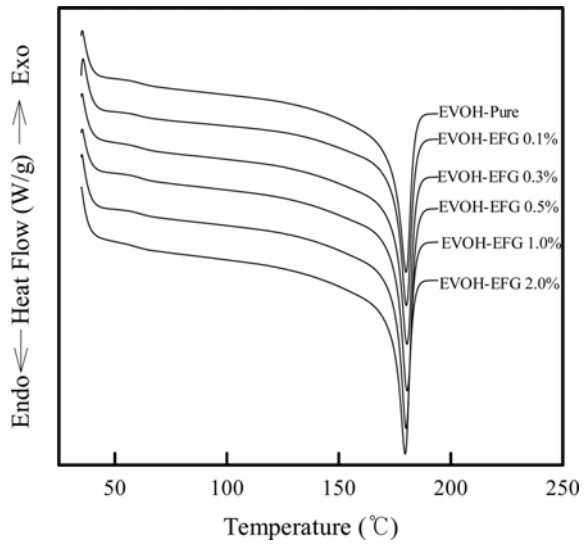

Figure 6. DSC curves of the EVOH/EGn nanocomposite films.

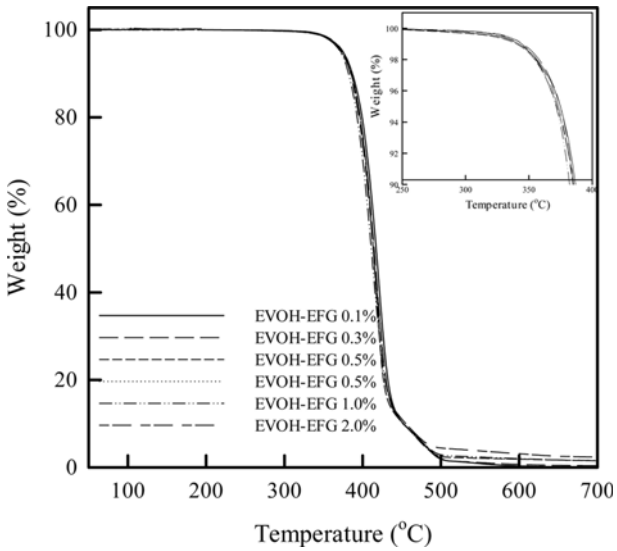

Figure 7. TGA curves of the EVOH/EGn nanocomposite films.

Table I. Thermal Properties of the EVOH/EGn Nanocomposite Films

Sample code	DSC			TGA	
	T_g[a] (°C)	T_m[a] (°C)	ΔH_m[a] (J/g)	$T_{3\%}$[b] (°C)	$T_{10\%}$[b] (°C)
Pure EVOH	61.6	180.0	72.1	359.5	381.3
EVOH/EGn 0.1%	61.0	180.2	72.2	364.7	386.9
EVOH/EGn 0.3%	61.5	180.5	73.1	365.4	385.4
EVOH/EGn 0.5%	61.6	180.5	77.7	362.2	385.3
EVOH/EGn 1.0%	61.9	180.1	72.5	362.4	382.3
EVOH/EGn 2.0%	60.3	179.6	73.6	363.7	384.5

[a]Glass transition temperature (T_g), melting temperature (T_m) and melting enthalpy (ΔH_m) were measured during 2nd heating after non-isothermal crystallization. [b]Decomposition temperatures at 3% and 10% weight loss of sample, respectively.

the EGn filler is not very large. Furthermore, on the basis of the enthalpies for melting, the melting enthalpy slightly increased up to 0.5 wt%, and decreased after this slight increase. However, the EVOH/EGn nanocomposite films showed relatively higher values than pure EVOH. This indicates that the crystallinity of EVOH in the EVOH/EGn nanocomposite films is slightly improved up to 0.5 wt%, probably because of the enhanced crystallization of EVOH on the surface of the EGn nanosheets. However, the nanocomposite films with relatively high EGn contents of 1 and 2% showed similar crystallinity as that of pure EVOH, which may come from poor dispersion of EGn. As evidenced by the FTIR, SEM, and WAXD analyses, there were no strong interactions between EVOH polymer chains and EGn, which may have hindered the enhancement of the thermal properties and crystallinity of the EVOH/EGn nanocomposite films.

TGA was performed to investigate the effects of EGn on the thermal stability of the EVOH/EGn nanocomposite films. As shown in Figure 7, pure EVOH showed a two-step degradation process. In the first step, a big weight loss occurred at about 360-450 °C, which may correspond to the structural decomposition of the polymers. The second step, at about 450-520 °C, should be due to the further decomposition of the remainder. Regardless of EGn content, however, five different EVOH/EGn nanocomposite films showed the same degradation process as pure EVOH, which indicates that the presence of the EGn particles does not significantly influence the thermal degradation patterns of the EVOH/EGn nanocomposite films. As summarized in Table I, all the EVOH/EGn nanocomposite films with EGn showed slightly higher decomposition temperatures than pure EVOH. The EGn particles have greater thermal stability than the polymer matrix and can physically confine the polymer chains, resulting in decreased polymer chain mobility. Therefore, it was anticipated that EGn loading in EVOH will increase the thermal stability in neat polymers. However, the increase in thermal stability by introducing EGn into EVOH is not as significant as expected from the high aspect ratio and their thermal stability. Weak interfacial interaction between EGn particles and EVOH may account for its low performance in terms of thermal properties.

Barrier Properties. Good gas and moisture barrier properties are critical for achieving a long protective period for packaged products.[1,31] The reduction of moisture sorption and diffusion can suppress internal damage and improve long-term performance. Therefore, barrier films must prevent or at least decrease the gas/moisture transfer between the product and the surrounding atmosphere. In this study, organic-inorganic nanocomposite films incorporating EGn with relatively high aspect ratio and high hydrophobicity were prepared by a solution blending method and their water vapor permeability and water uptake were investigated as a function of EGn content. The results are depicted in Figure 8 and Table II.

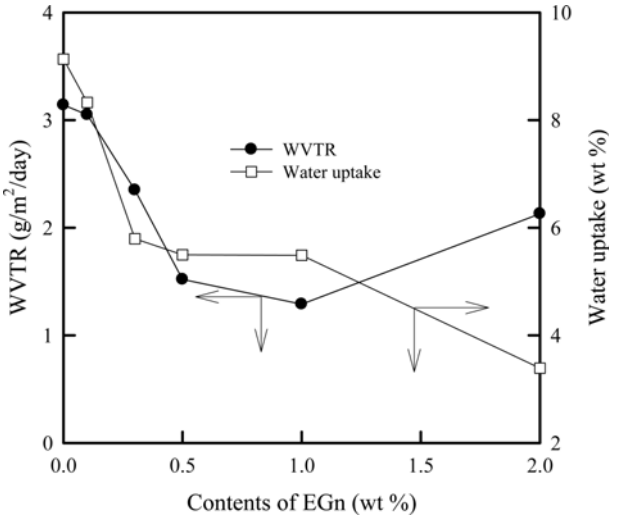

Figure 8. WVTR and water uptake of the EVOH/EGn nanocomposite films.

For the EVOH/EGn nanocomposite films, the WVTR varied in the range of 1.29 to 3.14 cc/m^2/day and apparently decreased up to 1% EGn loading and then increased slightly at 2% EGn loading. Furthermore, the water uptake changed from 9.1 to 3.4 wt%, greatly decreasing with increasing content of EGn particles. Overall, the WVTR and water uptake decreased as the EGn content increased. This indicates that the water resistance capacity of EVOH was greatly enhanced by the EVOH/EGn nanocomposite systems and moisture diffusion in the pure EVOH film was retarded by the incorporation of the EGn. It is well known that barrier properties and water sorption properties of materials indi-

Table II. Moisture Barrier Properties and Contact Angles of the EVOH/EGn Nanocomposite Films

Sample Code	WVTR (g/m^2·day)	Water Uptake (wt %)	Contact Angle (°)		
			at 0 s	at 500 s	Δ
Pure EVOH	3.2	9.1	68.2	57.8	10.4
EVOH/EFG 0.1%	3.0	8.3	76.7	65.7	11.0
EVOH/EFG 0.3%	2.4	5.8	87.3	78.9	8.4
EVOH/EFG 0.5%	1.5	5.5	90.8	83.4	7.4
EVOH/EFG 1.0%	1.3	5.5	95.5	90.4	5.1
EVOH/EFG 2.0%	2.1	3.4	102.0	97.1	4.9

cate their resistance to diffusion and sorption of substances and are highly dependent on both their chemical and morphological structures.[1,32,33]

To the point of chemical structure, the degree of hydrophobicity of a surface is an important factor for moisture barrier properties. Specifically, the water resistance of EGn particles consisting largely of carbon atoms is better than that of the EVOH matrix with a relatively hydrophilic hydroxyl group in the repeating unit. It is anticipated that loading EGn nanosheets will produce increased hydrophobicity in EVOH. The variation of contact angle by the filler loading will give insight into the behavior of the nanoparticles on the surface of the composite films and provide information regarding the hydrophobicity or hydrophilicity of the polymer matrix.[34] To investigate the surface properties of films originating from the different EGn contents, the water contact angles were measured at 23 ºC and 39% relative humidity, and their dependences on EGn content and time are depicted in Figure 9.

The initial contact angles are strongly dependent upon the content of EGn. The initial contact angle increased from 68.2º to 102.0º as the EGn content increased, which implies that the hydrophobicity of the pure EVOH film was greatly enhanced by increasing EGn content. In general, the changes in contact angle with time originate from the combined effect of the partial evaporation and the spreading/wetting process of the drop, resulting in a decrease in the contact angle.[35] As the environmental condition was controlled to maintain relatively high humidity (80%-90% relative humidity), the changes in contact angle may arise from the spreading and wetting process of the water drop. As shown in Figure 9, all the nanocomposite films with different contents EGn showed decreases in contact angles with increasing time.

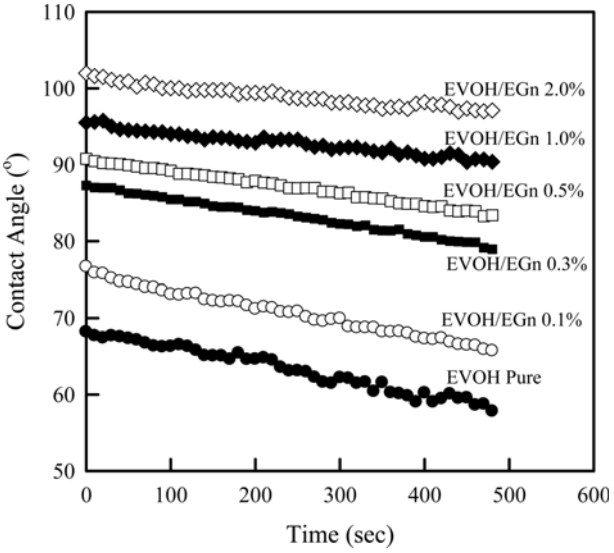

Figure 9. Time dependence of water contact angles for the EVOH/EGn nanocomposite films.

Depending on the content of EGn, the changes of contact angle with respect to time varied from 10.4 to 4.9, and apparently decreased as EGn content increased. This indicates that the loading of hydrophobic EGn will induce an increasingly hydrophobic surface and enhanced water resistance in pure EVOH films.

With good moisture barrier properties and large contact angles, water molecules find it difficult to dissolve in a polymer matrix, and therefore a relatively small amount of water molecules diffuse into the polymer matrix. This may be originated from enhanced hydrophobicity in EVOH by incorporating hydrophobic EGn nanosheets. As previously described in the DSC results, the EVOH/EGn nanocomposite films with EGn showed slightly enhanced molecular ordering and crystallinity in the amorphous and structure-less EVOH polymer. As crystalline regions are generally impermeable to the transport of low molecular substances, they may act as a barrier to water diffusion. Additionally, introducing EGn particles with a high aspect ratio into an EVOH film significantly complicates the path the water molecules would need to travel to pass through.[17,36] As shown in SEM results, however, the low content EGn particles are well dispersed throughout the matrix, whereas the high content EGn particles induce poor dispersion in EVOH matrix. As a result, this poor dispersibility may result in a slight increase in WVTR for EVOG/EGn 2% nanocomposite films. Therefore, further studies are needed to improve the performance of the moisture barrier properties by chemical treatment of graphite surface, decreasing the aspect ratio and optimizing the mixing method.[20,37,38]

Conclusions

Six different compositions of EVOH/EGn nanocomposite films were prepared from as-synthesized EGn nanosheets and EVOH, and their physical and moisture barrier properties were investigated as a function of the EGn content. The nanocomposite films prepared *via* a solution blending method showed no strong interactions between the polymer and EGn filler and resulted in poor dispersion in relatively high content EVOH/EGn nanocomposites. The thermal stability and glass transition are not enhanced by introducing EGn into EVOH. However, the water resistance capacity of EVOH was greatly enhanced and moisture diffusion in the pure EVOH film was retarded by introducing the EGn. The WVTR varied in the range of 1.29 to 3.14 cc/m^2/day, and apparently decreased up to 1% EGn loading. The water uptake greatly decreased from 9.1 to 3.4 wt % with increasing content of EGn particles. Thus, EGn particles with relatively high aspect ratio and hydrophobicity at the surface induced a slight increase in crystallinity and provided an efficient way to improve the moisture barrier properties of EVOH. To maximize their performance in nanocomposite films, however, further studies are required to increase the

compatibility and dispersion of EGn particles in the polymer matrix.

Acknowledgments. This work was supported by the Korea Foundation for the Advancement of Science & Creativity (KOFAC) grant funded by the Korean Government (MEST).

References

(1) S. M. E. Selke, J. D. Culter, and R. Z. Hernandez, *Plastic Packaging; Properties, Processing, Applications, and Regulations,* Hanser Gardner Publication, Munich, 2004.
(2) L. Cabedo, E. Gimenez, J. M. Lagaron, R. Gavara, and J. J. Saura, *Polymer,* **456**, 5233 (2004).
(3) H. M. Jeong, B. C. Kim, and E. H. Kim, *J. Mater. Sci.,* **40**, 3783 (2005).
(4) J. M. Lagaron and E. Nunez, *J. Plast. Film Sheet.,* **28**, 79 (2011).
(5) K. Kim, W. Sung, H. Park, Y. Lee, S. Han, and W. Kim, *J. Appl. Polym. Sci.,* **92**, 2069 (2004).
(6) T. V. Duncan, *J. Colloid Interface Sci.,* **363**, 1 (2011).
(7) J. Liang, Y. Huang, L. Zhang, Y. Wang, Y. Ma, T. Guo, and Y. Chen, *Adv. Funct. Mater.,* **19**, 1 (2009).
(8) C. Bao, Y. Guo, L. Song, and Y. Hu, *J. Mater. Chem.,* **21**, 13942 (2011).
(9) R. Sengupta, M. Bhattacharya, S. Bandyopadhyay, and A. K. Bhowmick, *Prog. Polym. Sci.,* **36**, 638 (2011).
(10) M. Xiao, L. Sun, J. J. Liu, Y. Li, and K. Gong, *Polymer,* **43**, 2245 (2002).
(11) G. Chen, D. Wu, W. Weng, D. Wu, and C. Wu, *Europ. Polym. J.,* **39**, 2329 (2003).
(12) F. M. Uhl, Q. Yao, H. Nakajima, E. Manias, and C. A. Wilkie, *Polym. Degrad. Stab.,* **89**, 70 (2005).
(13) K. Kalaitzidou, H. Fukushima, and L. T. Drzal, *Compos. Sci. Technol.,* **67**, 2045 (2007).
(14) A. Yasmi, J. Luo, and I. M. Daniel, *Compos. Sci. Technol.,* **66**, 1179 (2006).
(15) J. R. Potts, D. R. Dreyer, C. W. Bielawski, and R. S. Ruoff, *Polymer,* **52**, 5 (2011).
(16) T. Wei, Z. Fan, G. Luo, C.Zheng, and D. Xie, *Carbon,* **47**, 313 (2008).
(17) H. Kim, Y. Miura, and C. W. Macosko, *Chem. Mater.,* **22**, 3441 (2011).
(18) Y. Lee, D. Kim, H. Kwon, J. Seo, H. Han, and S. B. Khan, *Polym. Int.*, Accepted 2012.
(19) J. C. Wang, X. B. Wang, C. H. Xu, M. Zhang, and X. P. Shang, *Polym. Int.,* **60**, 816 (2011).
(20) D. W. Chae and B. C. Kim, *Polym. Adv. Technol.,* **16**, 846 (2005).
(21) E. Tang, H. Liu, L. Sun, E. Zheng, and G. Cheng, *Eur. Polym. J.,* **43**, 4210 (2007).
(22) H. B. Lee, A. V. Raghu, K. S. Yoon, and H. M. Jeong, *J. Macromol. Sci. Phys.,* **49**, 802 (2010).
(23) S. M. Oh, K. M. Oh, T. D. Dao, H. I. Lee, H. M. Jeong, and B. K. Kim, *Polym. Int.,* **62**, 54 (2012).
(24) M. Li and Y. G. Jeong, *Composites A,* **42**, 560 (2011).
(25) K. P. Pramoda, H. Hussain, H. M. Koh, H. R. Tan, and C. B. He, *J. Polym. Sci. Part A: Polym. Chem.,* **48**, 4262 (2010).
(26) B. J. Lee, *Bull. Korean Chem. Soc.,* **23**, 1801 (2002).
(27) G. Chen, D. Wu, W. Weng, and W. Yan, *J. Appl. Polym. Sci.,* **82**, 2506 (2001).
(28) T. Ramanthan, A. A. Abdala, S. Stankovich, D. A. Dikin, M. Herrera-Alonso, R. D. Piner, D. H. Admson, H. C. Schniepp, X. Chen, R. S. Ruoff, S. T. Nguyen, I. A. Aksay, R. K. Prud'homme, and L. C. Brinson, *Nat. Nanotechnol*, **3**, 327 (2008).
(29) J. C. Wang, X. B. Wang, C. H. Xu, M. Zhang, and X. P. Shang, *Polym. Int.,* **60**, 816 (2011).
(30) H. Kim and C. W. Macosko, *Polymer,* **50**, 3797 (2009).
(31) S. K. Bajpai, N. Chand, and V. Chaurasia, *J. Appl. Polym. Sci.,* **115**, 674 (2010).
(32) J. Seo H. Han, *Polym. Degrad. Stab.,* **77**, 477 (2002).
(33) L. Li, M. J. Liu, and S. Li, *Polymer,* **45**, 2837 (2004).
(34) S. T. Palakattukunnel, S. Thomas, P. A. Sreekumar, and S. Bandyopadhyay, *J. Polym. Res.,* **18**, 1277 (2011).
(35) Y. Yoshida, R. Sachdeva, and S. Miyazaki, *J. Mater. Sci. Mater. Med.,* **3**, 306 (1992).
(36) X. Shi and Z. Gan, *Eur. Polym. J.,* **43**, 4852 (2007).
(37) J. Li, J. K. Kim, and M. L. Sham, *Scr. Mater.*, **53**, 235 (2005).
(38) J. T. Choi, D. H. Kim, D. S. Ryu, H.I. Lee, H. M. Jeong, C. M. Shin, J. H. Kim, and B. K. Kim, *Macromol. Res.*, **19**, 809 (2011).